In vitro study of the antibacterial and anticancer activities of silver nanoparticles synthesized from Alpinia calcarata

Ruba Badarudheen
Govindaraju Rajalakshmi (raajeerajan@gmail.com)
Hindusthan College of Arts and Science
Mashhoor Kattali

Research Article

Keywords: Alpinia calcarata, AgNPs, green synthesis, antibacterial, anticancer

Posted Date: May 2nd, 2022

DOI: https://doi.org/10.21203/rs.3.rs-1589328/v1

Abstract

In recent years, plant-based nanoparticle synthesis and research attained significant attraction due to its potential biological application. Presently studies in bio-nanotechnology have attained fascinating attention due to the use of nanoparticles in various fields of life. We used aqueous leaf extract of *Alpinia calcarata* to synthesize silver nanoparticles (AgNPs) and characterized them using UV-vis spectra, scanning electron microscopy (SEM), Fourier transform infrared spectroscopy (FTIR), and other techniques. These AgNPs' antibacterial and anticancer properties were also investigated. SEM analysis depicted the uniformly distributed spherical nanoparticles with 20 to 22 nm size. EDX analysis revealed the presence of silver ions with a strong signal. Gram-positive and negative human pathogenic bacteria such as Methicillin-resistant *Staphylococcus aureus* (MRSA), *Escherichia coli (E. coli), Klebsiella pneumoniae* (*K. pneumoniae*), and *Pseudomonas aeruginosa* were inhibited by the synthesized AgNPs. Antibacterial activities of the AgNPs were directly proportional to the concentration. The diameter of the zone of inhibition of AgNPs on bacteria varies from species to species. AgNPs were also found to have anticancer action against the MFC7 human breast cancer cell line. The anticancer activity of synthesized AgNPs was directly proportional to the concentration. The IC50 of this AgNP on the MCF7 cell line was determined using a linear regression equation and found to be 219.64 µg/ml. Thus, *A. calcarata* aqueous leaf extract can be used to synthesize AgNPs in an eco-friendly manner, and these AgNPs can be used in anticancer and antibacterial medicines, food, and cosmetic industries after clinical studies.

1. Introduction

Nano-based research is significantly attractive in the modern era by showing this nano-sized particle's unique characteristics with various applications in various fields. Interestingly, the history of nanoparticles for human welfare is 100s years old, and it was first reported over 5000 years ago in Ayurvedic medicine. Currently, nanotechnology is considered the answer to several problems society faces. The primary reason for the progress of nanoscience and technology is its unique physical, chemical, and biological properties, compared to their bulk [1].

Advances in nanotechnology have opened new doors to fundamental and applied fields, such as improvements in the processing of nanoscale materials and the use of their physical, chemical, electronic, and optical properties. Nanotechnology-based products are unavoidable in almost every area of modern life. The nanoparticles have a significant role in cosmetics development, health industry, food industry, *etc*. Nanotechnology is used in environmental, medicinal, pharmacological, and gene therapy applications [2–4].

Chemical and physical procedures are commonly used to make nanoparticles, and the use of toxic compounds severely limits their therapeutic potential. As a result, developing a non-toxic, dependable, and environmentally acceptable method for synthesizing nanoparticles is critical to expanding their biological applications. Chemical processes can produce many nanoparticles with precise size and shape

in a shorter time. However, chemical synthesis is a time-consuming process that can generate hazardous by-products harmful to the environment and human health.

Bio nanotechnology combines biological concepts with chemical-physical techniques to create nanoparticles with specified properties and functionalities. It leads to a search for alternatives that could be eco-friendly and less toxic to humans and animals. A biological approach is one in which microbes and plants are used to protect or reducing agents. Biological agents such as bacteria, fungus, algae, and plants are commonly used in nanoparticle biosynthesis [5, 6]. The rate of metal ion reduction using biological agents is substantially faster, and it happens at medium pressure and temperature. Green nanoparticle synthesis with various plants and their extracts can be far more profitable and cost-effective than conventional biological synthesis processes involving bacteria such as *Bacillus subtilis* and fungi such as *Fusarium oxysporum* and *Penicillium sp.*

The nanoparticles' productivity using plants is highly beneficial because of their availability and wide distribution. Several experiments on synthesizing silver nanoparticles utilizing plants have also been conducted as *Sorghum bicolour, Oryza sativa Zea mays*, *Aloe vera*, *Medicago sativa, Cinnamon camphor*, *etc.* [7–10].

Silver-based nanoparticles require more attention than other metal nanoparticles because of their unique structure, size, magnetic, optical, and electrical properties. With a wide range of antibacterial, antioxidants, and anticancer applications, silver nanoparticles have piqued the interest of researchers and scientists. Silver nanoparticles can withstand a wide temperature range while maintaining low volatility compared to other nanoparticles.

The present study discussed the synthesis of bioactive silver nanoparticles using leaf extract of *Alpinia calcarata*. It is also called a snap Ginger, primarily found in India, and belongs to the family Zingiberaceae, a commonly available medicinal plant. In Ayurveda, Galanga (Sanskrit: rasna) is considered a Vata shamana drug known as (perarathai) in Tamil as a folk medicine for cold and sore throat.

This study aims to synthesize silver nanoparticles from aqueous leaf extract of *A. calcarata* and characterize the synthesized silver nanoparticles using UV visible spectroscopy, FTIR, SEM, and EDX. Antibacterial action against microorganisms that cause disease in humans like Methicillin-resistant *Staphylococcus aureus* (MRSA), *Klebsiella pneumonia, Pseudomonas aeruginosa*, and *Escherichia coli* was analyzed using these AgNPs. The anticancer activity of these AgNPs was also tested against the MCF7 human breast cancer cell line.

2. Materials And Methods

2.1. Collection and identification of the plant

Plant materials were collected from the Botanical Garden, University of Calicut (11°08'01.8"N 75°53'25.6"E). Dr. Pabhu K.M. (Senior Scientist, Centre for Medicinal Plant Research, Arya Vaidhyasala, Kottakkal, Kerala, India) identified the collected samples, and the voucher samples were deposited in the Herbarium with voucher number CMPR 10986. The plant's leaves were used for further studies.

2.2. Preparation of plant extract and Synthesis of AgNPs

The collected plant leaves were shade dried and powdered finely. Dried powder (1gm) was mixed in 100 ml sterile double distilled water (DDW), mixed thoroughly, and placed in a shaking incubator overnight. The mix was sieved using Whatman No.1 filter paper and kept at 4°C for storage. Plant extract (100 µl) was added to 10ml of 0.1mM $AgNO_3$ (Himedia) solution and agitated under normal pH. The brownish color in the solution is a vibrant indication of the establishment of silver nanoparticles in the reaction mixture. Silver nitrate solution without plant extract was also run along with experiment as control. To know the outcome of temperature on nanoparticles formation, the reaction mixtures were kept at different temperature like room temperature, 40°C, 50°C, and 60°C for 2 hours and observed the color change.

2.3. Characterisation of silver nanoparticles (AgNPs)

The synthesized AgNPs by reducing pure Ag + ions were diluted with distilled water (1:2 dilutions) and monitored the nanoparticle formation by measuring the UV-Vis spectrum using Shimadzu UV-1800 spectrophotometer. 0.1mM Silver nitrate was considered as blank. The Visible spectral analysis has been done from 350 to 600 nm.

Fourier Transform Infrared Spectroscopy (FTIR) was utilized in this study to depict the chemical composition of AgNPs synthesized using Jasco 4100 FTIR spectrophotometer from Dept. of Chemistry, University of Calicut. The lyophilized silver nanoparticles powder was pelletized with Potassium bromide (KBr) and characterized in the wavelength from 4000 – 400 cm^{-1}.

The procedure followed for observing silver nanoparticles by scanning electron microscopy using ZEISS Gemini SEM instrument- 300 connected to Octane Plus EDX system from Central Sophisticated Instrument Facility (CSIF) of University of Calicut. A drop of AgNPs was placed on a carbon-coated copper grid. The sample was prepared and subsequently dried in the air, which must have been done previously shifting to the microscope. The SEM was operated at a voltage of 120KV. EDX (Energy Dispersive analysis X-ray) was done, followed by SEM.

2.4. Antibacterial studies of AgNPs

The green synthesized AgNPs using *A. calcarata* extract were tested for antibacterial activity by agar well diffusion method against pathogenic bacteriae like Methicillin-resistant *Staphylococcus aureus* (MRSA), *Klebsiella pneumonia, Pseudomonas aeruginosa*, and *Escherichia coli.* The bacteria's pure culture (nutrient broth) was spread uniformly onto the individual nutrient agar plates. 10 mm diameter wells were made on nutrient agar using gel puncture, and 20 µl of the nanoparticle sample in deferent concentrations (10µg, 20 µg, 40 µg, 80 µg, and 100 µg/ ml) were dispensed into each well. After overnight incubation at 37°C, the zone of inhibition of bacteria was measured.

2.5. Anticancer activity study using MTT assay

MCF7 breast cancer cell line was used to determine the anticancer activity of synthesized AgNPs. About 20,000 cells/well (200µl of MCF7 cell suspension) were added to each well of the 96-well plate. Then the cells were cultured in a Co_2 incubator for 24 hours. Different concentrations (12.5, 25, 50, 100, and 200 µg/ml) of AgNPs solutions were prepared in sterile double distilled water. These nanoparticles solutions were added to the different wells. Cells in a well without any drug were used as a negative control, and Camptothecin (25µM) was used as a positive control. The culture was kept in a Co_2 incubator at 37°C for 24 hours. The direct examination of nanoparticles treated and untreated MCF7 cells were recorded with an inverted microscope. After incubation, removed the media and treated the cells with MTT reagent to a final concentration of 0.5 mg/ml of total volume. The plates were covered to avoid sunlight exposure. Incubated the plate for 3 hours and removed the MTT reagent after incubation. Then added, solubilization agent DMSO (100 µl) to the wells. The plates were stirred gently using a gyratory shaker to enhance dissolution. Absorbance was checked at 570nm in a UV- Spectrophotometer using DMSO as the blank. The following formula determined cell survival.

Viability % = (Test OD/ Control OD) X 100

Cytotoxicity % = 100 – Viability%

The IC50 value was determined by using a linear regression equation. *i.e.* Y = Mx + C.

Y = 50, M, and C values were derived from the viability graph.

3. Results And Discussion

3.1. Synthesis

The AgNPs were synthesized by *A. calcarata* aqueous leaf extract. The AgNPs synthesis initially confirmed by the change of color of the reaction blend from colorless to brown was observed. The temperature effect on the synthesis was also depicted. Transformation in the color of the reaction mixture was different at varying temperatures (Fig. 1). Usually, the silver ion solutions are colorless; when the silver ions are reduced by plant extract, it turns the color brown. Studies suggested that phytochemicals such as phenols, proteins, and flavonoids are essential in reducing Ag + ions [11]. Phytochemicals such as carboxylic acids, phenols, alkaloids, triterpenoids, and steroids may be present in plants which may be helpful for the synthesis of nanoparticles. In earlier studies, Oves *et al*. [12] and Pirtarighat *et al*. [13] testified the relevance of plant metabolites in the synthesis and stabilization of green synthesized nanoparticles. The transformation in the color of the reaction mixture is due to the excitation of the surface plasmon resonance (SPR) formed due to the reduction of Ag + ions to AgNPs [14].

3.2. UV–vis spectrum study of AgNPs

The spectrophotometric analysis of synthesized AgNPs revealed the maximum peak between 420-450nm (Fig. 2). Thangaraju et al. [15] showed that AgNPs exhibit UV-visible absorption maxima at 400-500nm in a previous study. The confirmation of AgNPs synthesis by UV-visible spectra is because of the excitation of the SPR [15]. Increased optical density indicates the amount of AgNPs synthesized. Temperature also showed a significant effect on the synthesis of AgNPs. There is a considerable rise in the absorbency of AgNPs with the increase in temperature. The amount of AgNPs synthesized (OD) at room temperature is less than at the higher temperature. The previous studies also revealed that efficient synthesis of AgNPs occurs at higher temperatures [16, 17]. Udayasoorian *et al.* [18] and Usha *et al*. [19] also established that the production of AgNPs usually increases with the increase in temperature.

In spectrophotometer analysis, the variation in absorption peak at varying temperatures is also noted. The maximum absorbency wavelength of each temperature showed variation. The maximum absorbency of AgNPs synthesized in 60°C was recorded at 431nm wavelength. Whereas maximum absorbency of AgNPs synthesized at 50°C, 40°C, and the room temperature was recorded at 423nm, 419nm, and 422nm, respectively. The absorption peak shifts from one wavelength to another at different temperatures can be owing to the localization of the SPR of the AgNPs [20].

3.3. FTIR analysis

The FTIR was used to detect different functional groups of AgNPs synthesized using *A. Calcarata*. The FTIR spectra of the AgNPs synthesized are presented in Fig. 3. A peak in 3418.21cm^{-1} was observed, corresponding to a broad O-H stretching. A stretching Alkyl C-H and Alkene **C = C** vibration band were detected at 2923.56 cm^{-1} and 1615.09 $cm^{-1,}$ respectively. Two deformation vibration peaks of C-H were also recorded in energy regions 1383.11cm^{-1} and 1311.36 cm^{-1}. The functional groups identified in this present study may be involved in the synthesis or stabilization of AgNPs synthesized.

3.4. SEM and EDX Analysis

SEM analysis revealed the size and shape of the AgNPS synthesized using *A. calcarata* leaf extract. EDX experiment depicted the presence of elemental silver in AgNPs synthesized. The SEM image of AgNPs synthesized by *A. calcarata* showed uniformly distributed spherical AgNPs. The average size of spherical AgNPs arrays is 20–22 nm (Fig. 4). The image also showed the aggregation of AgNPs.

The chemical analysis of AgNPs (crystal) synthesized by *A. calcarata* was analyzed by Energy-dispersive X-ray spectroscopy (EDX). A strong signal of silver was observed with weak signals of Cl in EDX (Fig. 5).

3.5. Antibacterial activity of AgNPs synthesized by *A. calcarata*

Well diffusion method reveals the potent antibacterial activity of AgNPs synthesized by *A. calcarata* (Table 1, Fig. 6). The nanoparticles synthesized by this plant exhibit a significant effect on the selected pathogenic bacteria like MRSA, *K. pneumonia, E. coli*, and *P. aeruginosa*. This study indicates that the concentration of AgNPs has a major role in increasing or decreasing the inhibitory effect on bacteria. The

zone of inhibition of AgNPs on MRSA at varying concentrations was found to be 4mm, 5mm, 6mm, 8mm, and 10mm at 10 µg/ml, 20 µg/ml, 40 µg/ml, 80µg/ml and 100 µg/ml respectively. At the concentration of 10 µg/ml, 20 µg/ml, 40 µg/ml, 80µg/ml, and 100µg/ml, these synthesized AgNPs showed 3mm, 4mm, 6mm, 7mm, and 8mm zone of inhibition on *K. pneumonia*. Zone of inhibition against *E. coli* was recorded as 5mm, 5mm, 7mm,10mm, and 12mm at 10 µg/ml, 20 µg/ml, 40 µg/ml, 80µg/ml, and 100µg/ml concentration of AgNPs synthesized by *A. calcarata*. Whereas *P. aeruginosa* showed 2mm, 3mm, 6mm, 7mm and 9mm zone of inhibition at 10 µg/ml, 20 µg/ml, 40 µg/ml, 80µg/ml and 100µg/ml concentration of AgNPs. The high concentration of nanoparticles exhibited increased inhibition as low concentration showed less effect. The antibacterial effect of AgNPs synthesized by *A. calcarata* has a varying effect on different bacteria, and it was interesting that AgNPs synthesized by *A. calcarata* have a significant effect on MRSA.

Table 1
Antibacterial activity of green synthesized AgNPs using *A. calcarata*

Bacteria	Zone of inhibition (mm)				
	10µg/ml	20µg/ml	40µg/ml	80µg/ml	100µg/ml
MRSA	4	5	6	8	10
K. pneumonia	3	4	6	7	8
E. coli	5	5	7	10	12
P. aeruginosa	2	3	6	7	9

In recent years, the biosynthesis of AgNPs achieved great attention compared to chemical and physical methods for antimicrobial activity studies. Like this present study, many earlier studies have suggested the possible use of nanoparticles to control the growth of various bacteria, including pathogenic bacteria. AgNPs are characterized by which provide better contact with the bacterial membrane [21], which may make these particles to penetrate the cells or do direct damage to the cells. The nanoparticles can be highly harmful to the bacterial cell, and the antibacterial property of the AgNPs was found to be significantly augmented in response to the decrease in size [22]. The efficient antibacterial activity of the AgNPs synthesized in this study may be due to their small size. The antibacterial activity of synthesized AgNPs increased with respect to the rise in concentration. The result of this study is supported by the previous study conducted by Kim *et al*. [23]. Mechanism of antibacterial activity of AgNPs attained significant attention in bionanotechnology. Several mechanisms of action were reported to explain the mode of action of AgNPs. The most credible mechanism was the establishment of free radicals by the action of AgNPs. In living cells, free radicals assaults lipids found in the membrane, which primes to the dissociation of membrane lipids, damage finally, the growth of cells will be inhibited [24].

3.7 Anticancer activity

The anticancer activity of synthesized AgNPs showed a remarkable effect on the MCF7 cell line. Table 2 shows the inhibition and cell viability of AgNPs treated MCF7 cells. The activity of synthesized AgNP was

found to be high in increased concentration. The cytotoxic activity of AgNPs synthesized by *A. calcarata* was unswervingly proportionate to the concentration (Fig. 7). The cell inhibition of AgNPs at different concentrations was found to be 1.46%, 11.64%, 23.41%, 32.95% and 42.05 at 12.50 µg/ml, 25 µg/ml, 50 µg/ml, 100 µg/ml and 200 µg/ml respectively. The IC50 of AgNP on the MCF7 cell line was determined using a linear regression equation and found to be 219.64 µg/ml. The microscopic image of the MCF7 cell line also depicted the cytotoxic effect of AgNPs synthesized by *A. calcarata* (Fig. 8).

Table 2
Cytotoxic effect of green synthesized AgNPs using *A. calcarata* on MCF cell line

Concentration of AgNPs µg/ml	% Cell viability	% Cell inhibition
12.5	98.54	1.46
25	88.36	11.64
50	76.59	23.41
100	67.05	32.95
200	57.95	42.05
Cell Control	**100.00**	**0.00**
Std Control	**50.13**	**49.87**

Studies reveal that it is essential to develop an alternative strategy to control cancer globally due to the alarming side effect of current chemotherapeutic medicines. Many researchers have described the use of nanoparticles for controlling the growth of cancer in *in vitro* studies. AgNP synthesized from *Taraxacum officinalis* and *Commelina nudiflora* expressed toxicity on human liver cancer cells and colon cancer cells respectively [25, 26]. The AgNP synthesized in this study with *A. calcarata* has a significant effect on human breast cancer cell line MCF7, which conforms with the anticancer activity of AgNPs synthesized by chemical means [27].

The cytotoxicity of AgNP was found to be concentration depended [28]. The AgNPs synthesized in this study also showed an increased effect in high concentration were as in lower concentration, activity was less. The cytotoxic effect AgNPs on MCF7 cells can be attributable to the release of Ag + ions that can bind with the cell membrane and cellular protein and DNA. These AgNPs can cause DNA damage [29] and increased membrane permeability of mitochondria [30]. The cytotoxicity of AgNPs was suggested to be created through the increased reactive oxygen species (ROS) level. During the exposure of cells to AgNPs, Kim and Ryu [31] have recorded an increased level of apoptosis, enhancement in oxidative stress, and genotoxicity. The increased intracellular ROS react with protein and root oxidative stress [32], which will prime to the temporary or eternal injury of the structure or function of cellular proteins. Apart from the increased ROS level generation, the AgNPs negatively regulate the activity of a key enzyme (DNA-dependent protein kinase) involved in DNA damage repair via nonhomologous end joining.

4. Conclusions

The current study reports the synthesis of AgNPs with aqueous leaf extract of *A. calcarata*. The establishment of nanoparticles was confirmed by transforming the color of the solution from colorless to brown. The optimum temperature for the production of AgNPs via aqueous leaf extract of *A. calcarata* was 60°C, and the temperature has unswervingly proportional to the formation of AgNPs. The present study revealed the uniformly distributed spherical structure of AgNPs with the size of 20-22nm in SEM images. EDX analysis suggested the presents of Ag + ions as a significant signal in AgNPs synthesized by *A. calcarata*. FTIR study depicted the functional groups existing in these AgNPs. In this present study, the potential antibacterial property of this AgNP against human pathogenic bacteria MRSA, *K. pneumonia, E. coli*, and *P. aeruginosa* were revealed. These green synthesized AgNPs were active on MCF7 cell line with IC50 at 219.64 µg/ml concentration. Because of the significant antibacterial and anti-cancer activity of these AgNPs synthesized by *A. calcarata* can be used in medicines, food, and cosmetic industries after the clinical studies.

Abbreviations

AgNPs
silver nanoparticles
SEM
scanning electron microscopy
FTIR
fourier transform infrared spectroscopy
EDX
energy dispersive analysis X-ray
MRSA
methicillin-resistant *Staphylococcus aureus*
DDW
double distilled water
$AgNO_3$
silver nitrate
Ag+
silver ion
MTT
3-(4,5-dimethylthiazol-2-yl)-2,5-diphenyl tetrazolium bromide
DMSO
dimethyl sulfoxide
SPR
surface plasmon resonance
OD

optical density

Declarations

Acknowledgments

None

Funding

This research did not receive any specific grant from funding agencies in public, commercial, or not-for-profit sectors.

Conflict of Interest

None

References

1. A.R. Ingole, S.R. Thakare, N.T. Khati, Chalcogenide Lett. **7**, 485 (2010)
2. F.K. Alanazi, A.A. Radwan, I.A. Alsarra, Saudi Pharm. J. **18**, 179 (2010)
3. E. Rodríguez-Carmona, A. Villaverde, Trends Microbiol. **18**, 423 (2010)
4. A.N. Misra, M. Misra, R. Singh, Int. J. Pure Appl. Sci. Technol. **16**, 9 (2013)
5. M.K. Rai, S.D. Deshmukh, A.P. Ingle, A.K. Gade, J. Appl. Microbiol. **112**, 841 (2012)
6. G. Li, D. He, Y. Qian, B. Guan, S. Gao, Y. Cui, K. Yokoyama, L. Wang, Int. J. Mol. Sci. **13**, 466 (2011)
7. S.P. Chandran, M. Chaudhary, R. Pasricha, A. Ahmad, M. Sastry, Biotechnol. Prog **22**, 577 (2006)
8. J.L. Gardea-Torresdey, E. Gomez, J.R. Peralta-Videa, J.G. Parsons, H. Troiani, and M. Jose-Yacaman, Langmuir **19**, 1357 (2003)
9. D. Gnanasangeetha, D. SaralaThambavani, Desalin. Water Treat **56**, 1839 (2015)
10. R. Perveen, F. Islam, J. Khanum, T. Yeasmin, Asian Pac. J. Trop. Med. **5**, 121 (2012)
11. N. Ahmad, S. Sharma, V.N. Singh, S.F. Shamsi, A. Fatma, B.R. Mehta, Biotechnol. Res. Int. 2011, e454090 (2010)
12. M. Oves, M. Aslam, M.A. Rauf, S. Qayyum, H.A. Qari, M.S. Khan, M.Z. Alam, S. Tabrez, A. Pugazhendhi, I.M.I. Ismail, Mater. Sci. Eng. C Mater. Biol. Appl. **89**, 429 (2018)
13. S. Pirtarighat, M. Ghannadnia, S. Baghshahi, J. Nanostructure Chem. **9**, 1 (2019)
14. C. Krishnaraj, E.G. Jagan, S. Rajasekar, P. Selvakumar, P.T. Kalaichelvan, N. Mohan, Colloids Surf. B Biointerfaces **76**, 50 (2010)
15. D. Philip, Spectrochim. Acta. A. Mol. Biomol. Spectrosc. **78**, 327 (2011)
16. S. Gnanasekar, G. Chandrakasan, K. Karpagam, H. Vedagiri, K. Premkumar, S. Sivaramakrishnan, Colloids Surf. B Biointerfaces **95**, 235 (2012)

17. R. Sukirtha, K.M. Priyanka, J.J. Antony, S. Kamalakkannan, R. Thangam, P. Gunasekaran, M. Krishnan, S. Achiraman, Process. Biochem. **47**, 273 (2012)
18. C. Udayasoorian, K.V. Kumar, R.M. Jayabalakrishnan, Digest J. Nanomater. Biostrut. 279 (2011)
19. P. Usha Rani, P. Rajasekharreddy, Colloids Surf. **389**, 188 (2011)
20. 20M.A. Fayaz, K. Balaji, P.T. Kalaichelvan, R. Venkatesan, Colloids Surf. B Biointerfaces **74**, 123 (2009)
21. M. Rai, A. Yadav, A. Gade, Biotechnol. Adv. **27**, 76 (2009)
22. S. Agnihotri, S. Mukherji, S. Mukherji, RSC Adv. **4**, 3974 (2013)
23. D.H. Kim, J.C. Park, G.E. Jeon, C.S. Kim, J.H. Seo, Biotechnol. Bioprocess. Eng. **22**, 210 (2017)
24. E. Mendis, N. Rajapakse, H.-G. Byun, S.-K. Kim, Life Sci. **77**, 2166 (2005)
25. R.G. Saratale, G. Benelli, G. Kumar, D.S. Kim, G.D. Saratale, Environ. Sci. Pollut Res. Int. **25**, 10392 (2018)
26. P. Kuppusamy, S.J.A. Ichwan, P.N.H. Al-Zikri, W.H. Suriyah, I. Soundharrajan, N. Govindan, G.P. Maniam, M.M. Yusoff, Biol. Trace Elem. Res. **173**, 297 (2016)
27. N.E.-A. El-Naggar, M.H. Hussein, A.A. El-Sawah, Sci. Rep. **7**, 10844 (2017)
28. A. Melaiye, R.S. Simons, A. Milsted, F. Pingitore, C. Wesdemiotis, C.A. Tessier, W.J. Youngs, J. Med. Chem. **47**, 973 (2004)
29. W. Wang, T. Kirsch, J. Biol. Chem. **281**, 30848 (2006)
30. M.R. Almofti, T. Ichikawa, K. Yamashita, H. Terada, Y. Shinohara, J. Biochem. (Tokyo) **134**, 43 (2003)
31. S. Kim, D.-Y. Ryu, J. Appl. Toxicol. JAT **33**, 78 (2013)
32. M.F. Rahman, J. Wang, T.A. Patterson, U.T. Saini, B.L. Robinson, G.D. Newport, R.C. Murdock, J.J. Schlager, S.M. Hussain, S.F. Ali, Toxicol. Lett. **187**, 15 (2009)

Figures

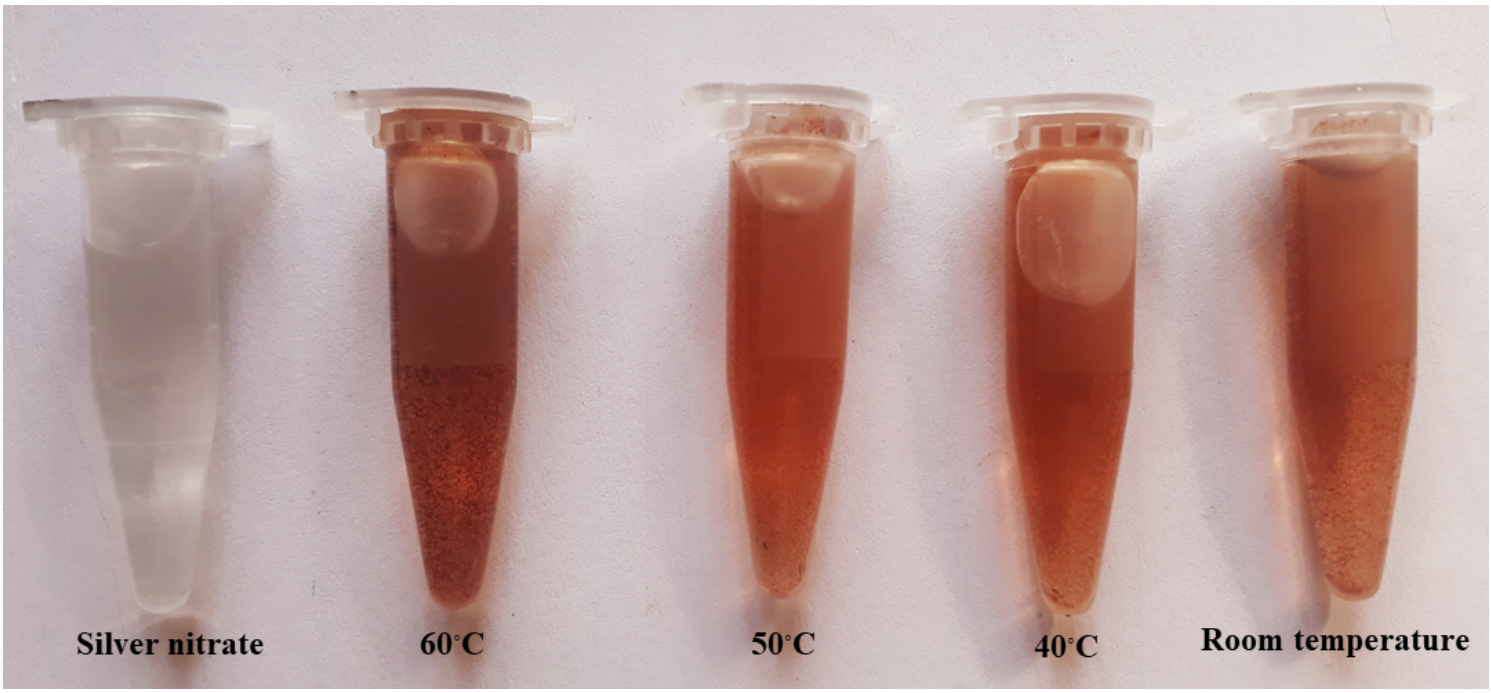

Figure 1

AgNPs synthesized using *A. calcarata* at different temperatures

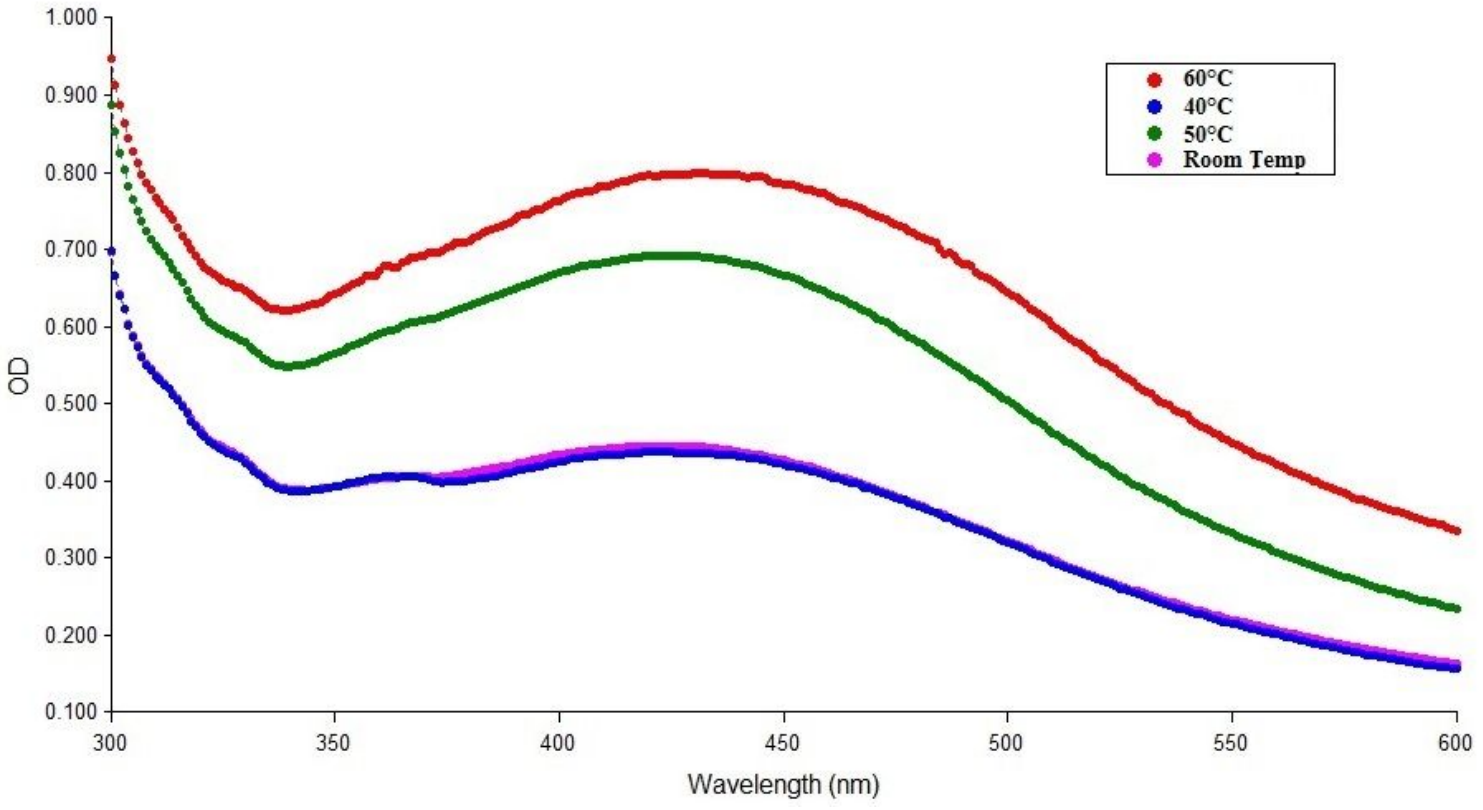

Figure 2

UV–vis spectrum analysis of AgNPs synthesized by A. Calcarata at different temperatures

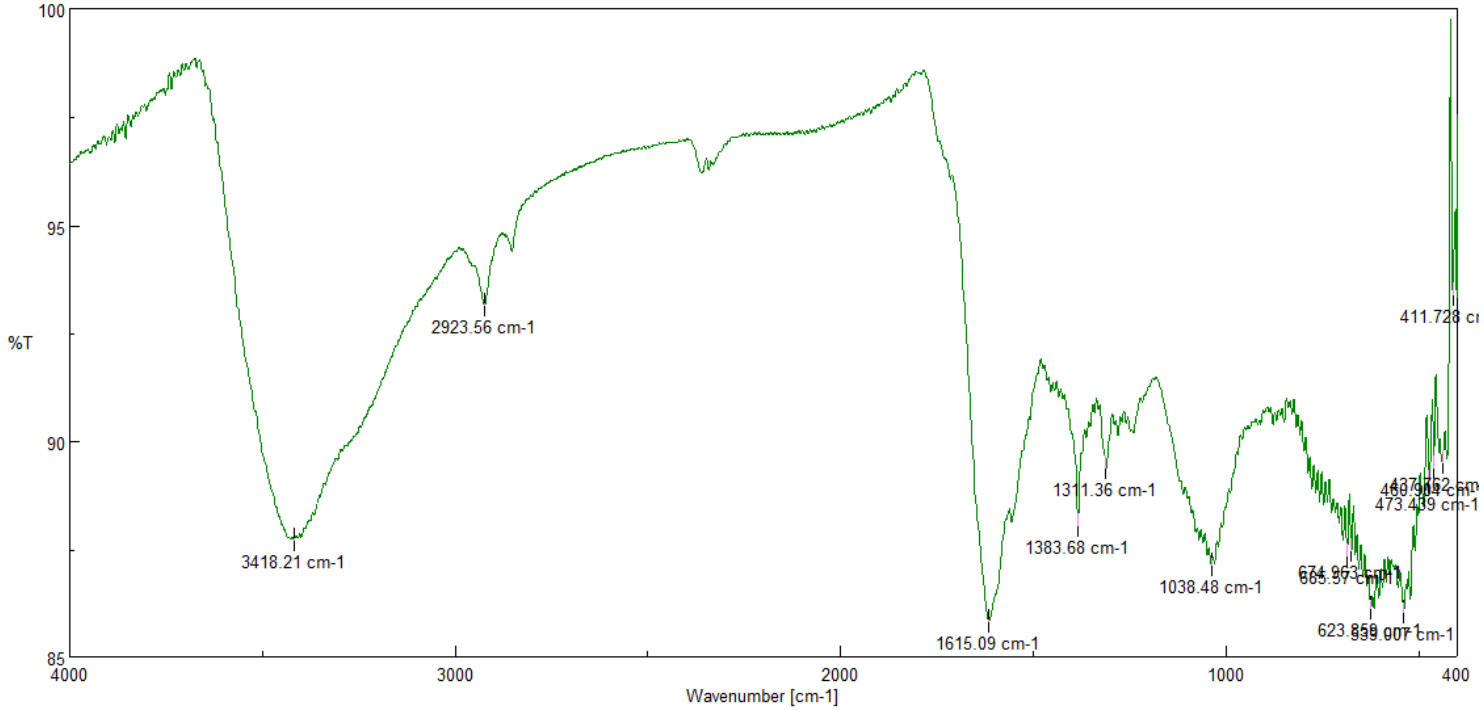

Figure 3

FTIR Spectroscopy analysis of AgNPs showing the occurrence of distinct functional groups.

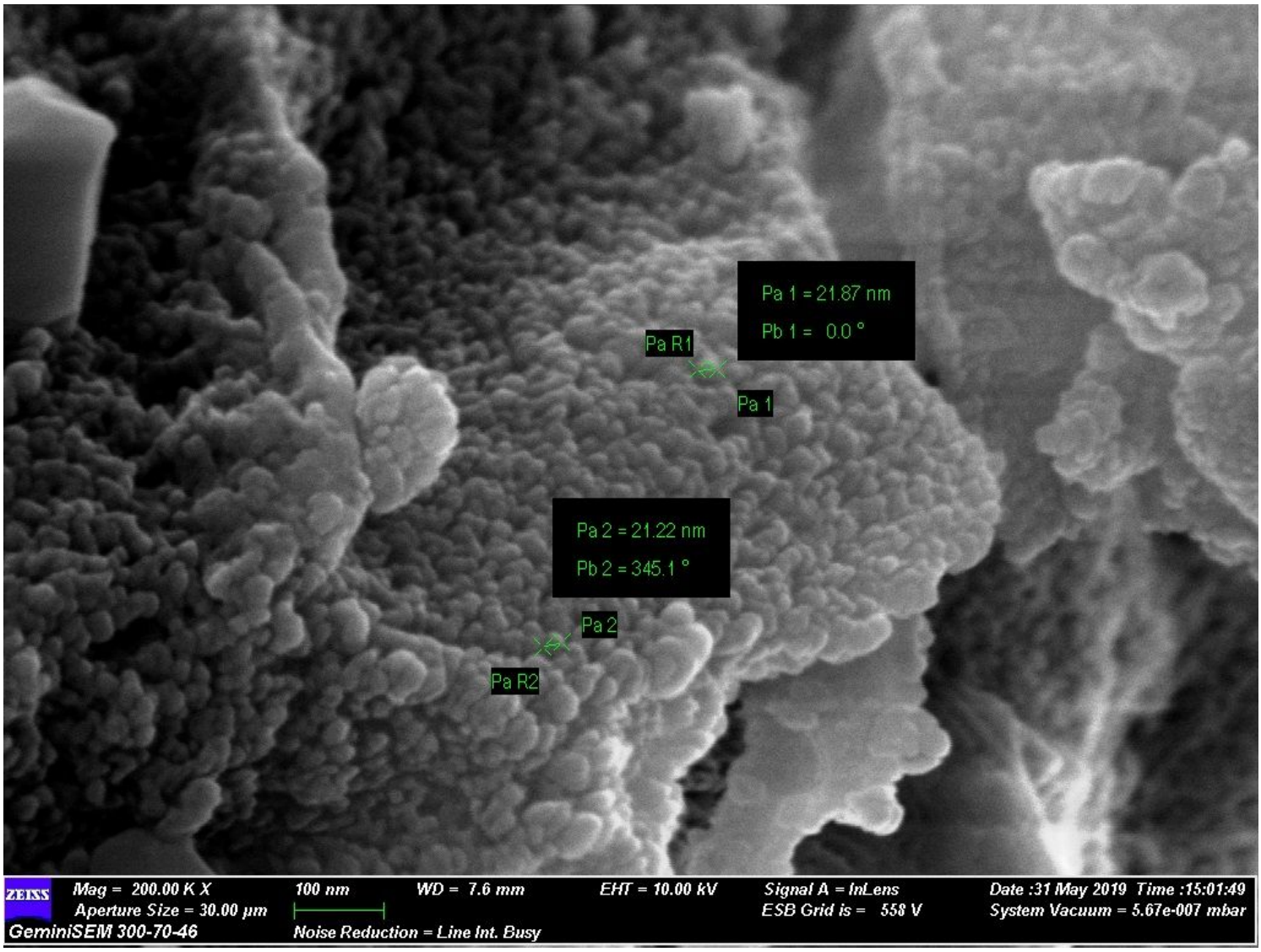

Figure 4

The SEM image shows the *AgNPs (spherical) synthesized by A. calcarata*

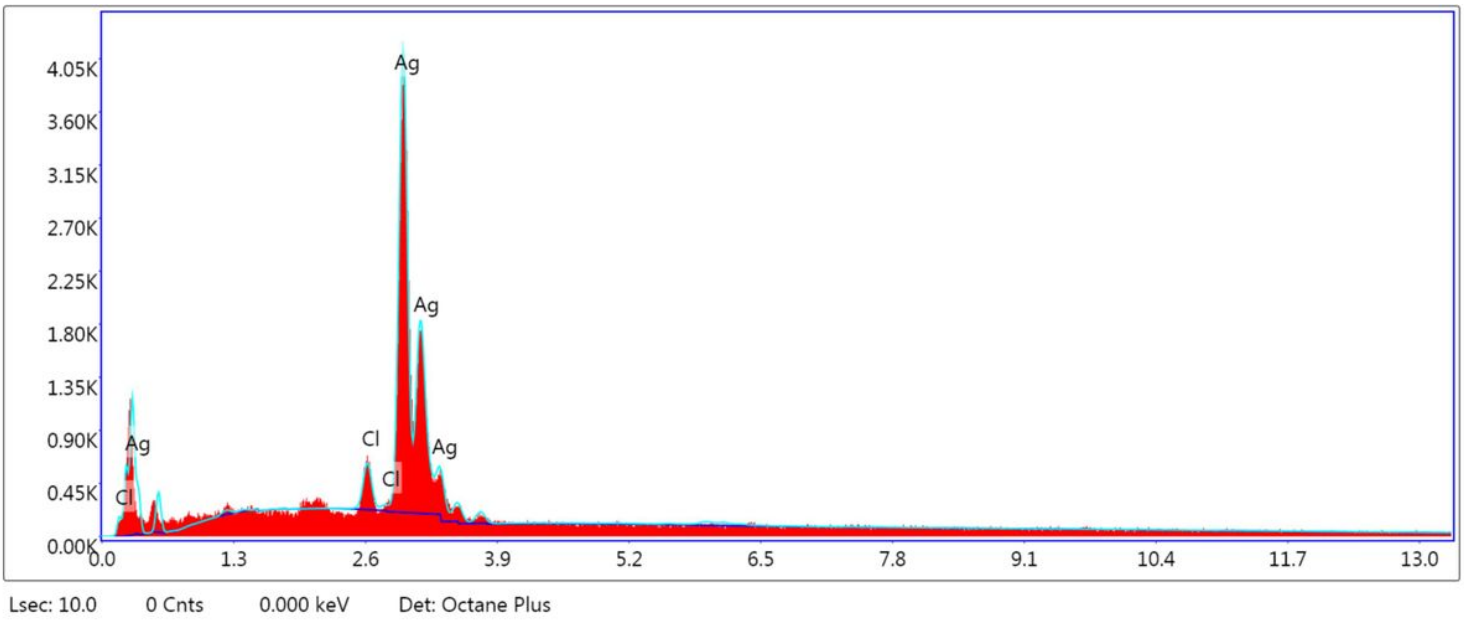

Figure 5

EDX analysis of *AgNPs synthesized by A. calcarata*

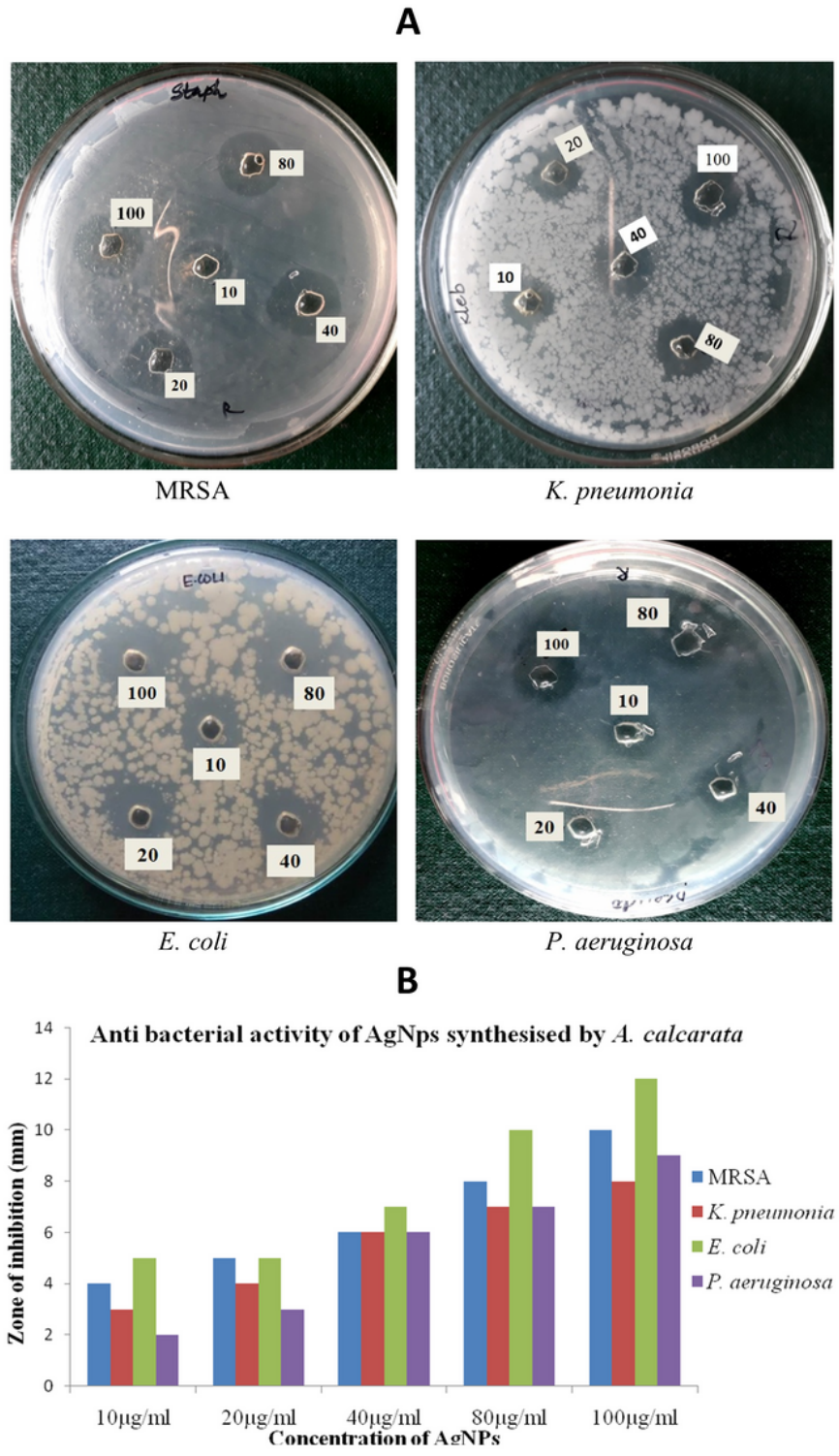

Figure 6

(A) Antibacterial property of AgNPs synthesized by *A. calcarata* against pathogenic bacteria. **(B)** Graph showing antibacterial activity of green synthesized AgNPs using *A. calcarata*

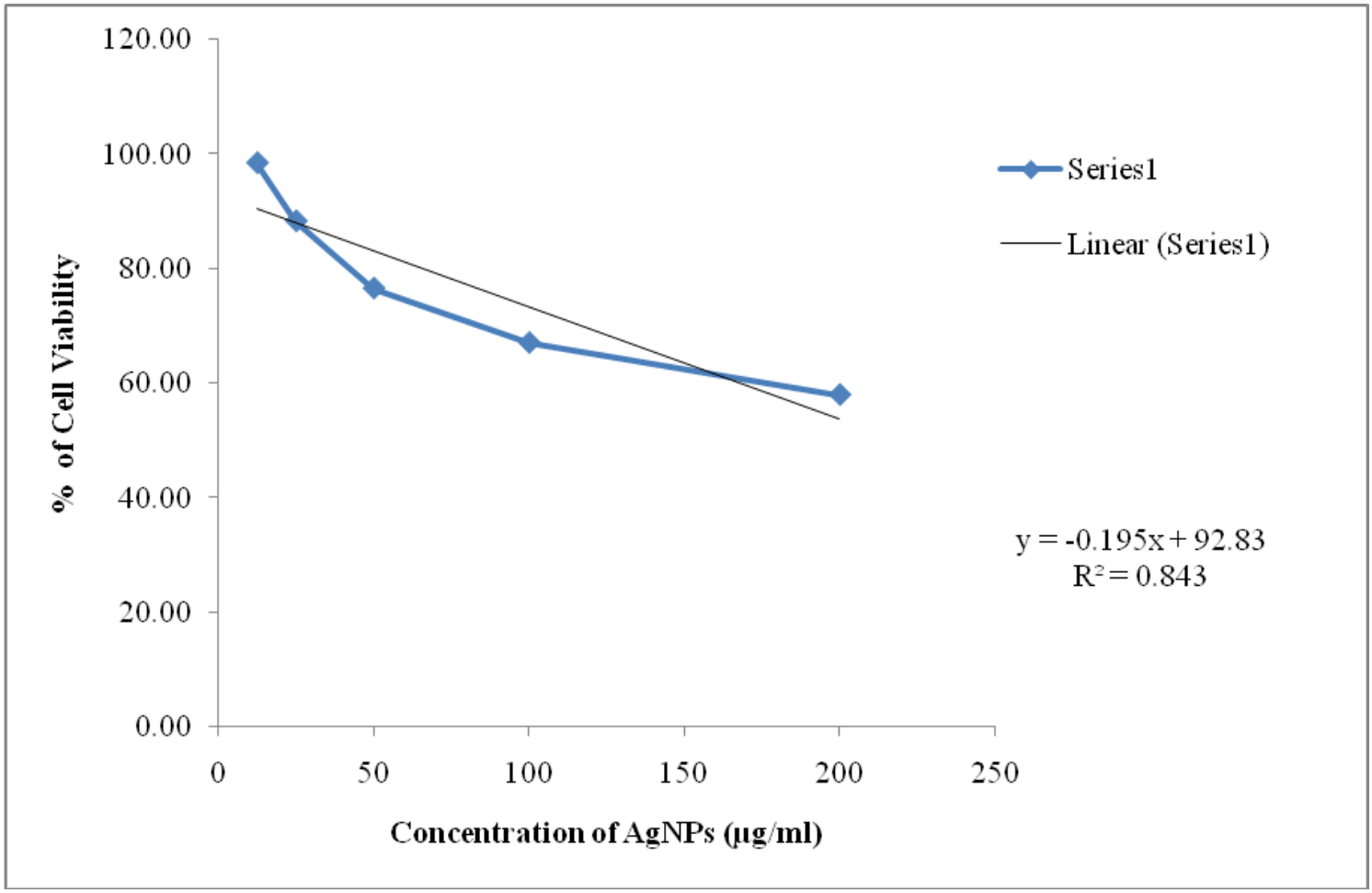

Figure 7

Cytotoxic effect of green synthesized AgNPs on MCF7 cell line

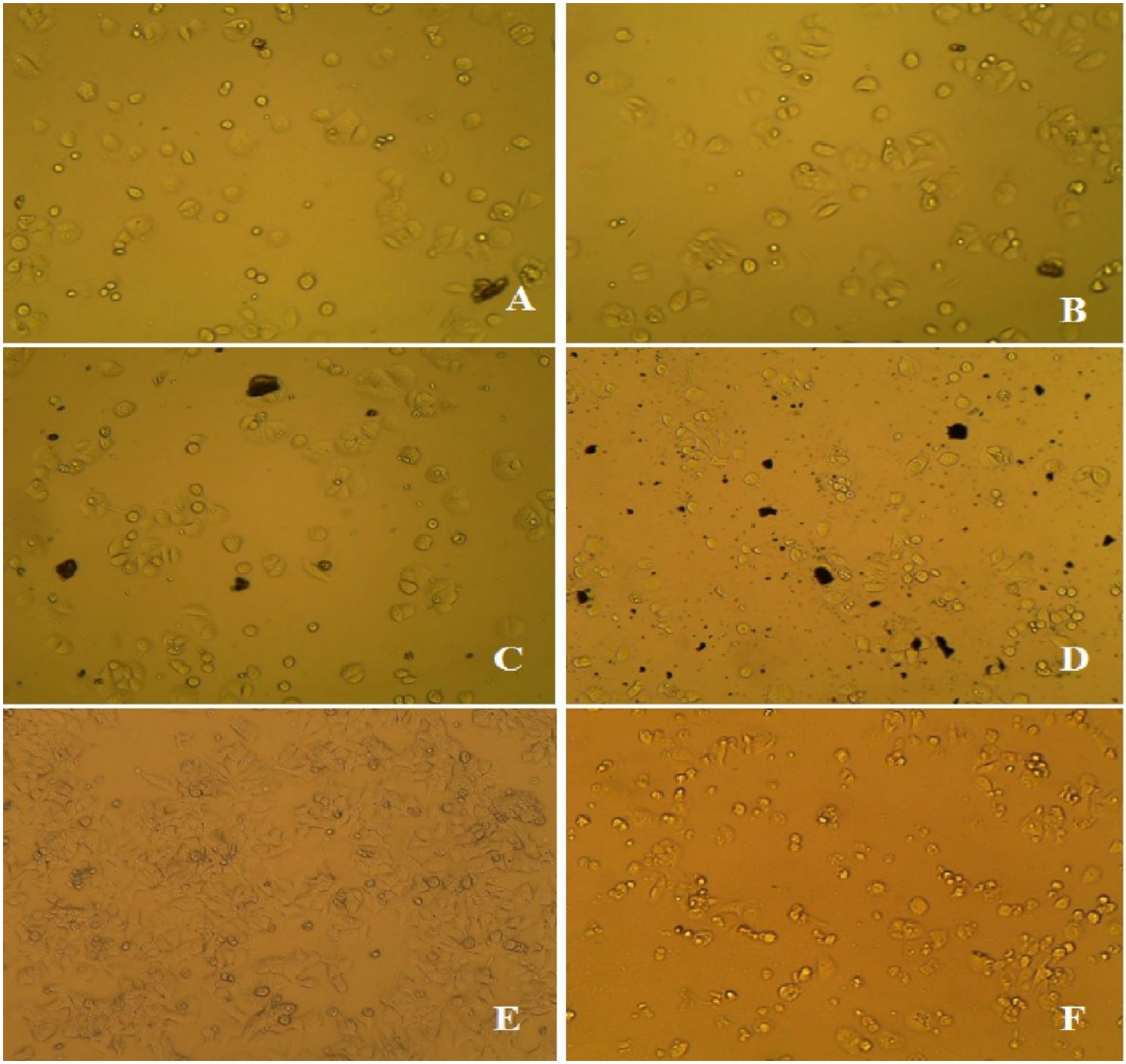

Figure 8

Microscopic images of the treated and untreated MCF7 cell line. **A.** AgNP (25µg/ml), **B** AgNP (50µg/ml)**, C** AgNP (100 µg/ml)**, D** AgNP (200µg/ml)**, E.** untreated**, F.** Camptothecin (positive control).